APPROVED FOR PUBLIC RELEASE; DISTRIBUTION UNLIMITED.

ENSEC, INC.

80 10 6 046

APPROVED FOR PUBLIC RELEASE, DISTRIBUTION UNLIMITED

SAR(01)-TR-79-05
10 December 1979

INTERACTIVE AND AUTOMATIC MODES OF LONG-PERIOD SIGNAL EXTRACTION USING CASCADED FILTERS

TECHNICAL REPORT NO. 5

PREPARED BY

ALAN C. STRAUSS

PREPARED FOR

AIR FORCE TECHNICAL APPLICATIONS CENTER
ALEXANDRIA, VIRGINIA 22314

ENSCO, INC.
SEISMIC APPLIED RESEARCH DIVISION
813 NORTH ROYAL STREET
ALEXANDRIA, VIRGINIA 22314

UNCLASSIFIED

SECURITY CLASSIFICATION OF THIS PAGE (When Data Entered)

REPORT DOCUMENTATION PAGE

READ INSTRUCTIONS BEFORE COMPLETING FORM

1. REPORT NUMBER

2. GOVT ACCESSION NO. AD-A089994

3. RECIPIENT'S CATALOG NUMBER

4. TITLE (and Subtitle)

(6) INTERACTIVE AND AUTOMATIC MODES OF LONG-PERIOD SIGNAL EXTRACTION USING CASCADED FILTERS,

5. TYPE OF REPORT & PERIOD COVERED

(9) Technical rept.,

6. PERFORMING ORG. REPORT NUMBER

(14) SAR(01)-TR-79-05

7. AUTHOR(s)

(10) Alan C. Strauss

8. CONTRACT OR GRANT NUMBER(s)

(15) F08606-79-C-0014, ARPA Order-2551

9. PERFORMING ORGANIZATION NAME AND ADDRESS

ENSCO, INC.
SAR Division
Alexandria, Virginia 22314

10. PROGRAM ELEMENT, PROJECT, TASK AREA & WORK UNIT NUMBERS

VELA T/9705/B/PMP

11. CONTROLLING OFFICE NAME AND ADDRESS

Advanced Research Projects Agency
Nuclear Monitoring Research Office
Arlington, Virginia 22209

(11) 12. REPORT DATE

10 December 1979

13. NUMBER OF PAGES

69 (12) 72

14. MONITORING AGENCY NAME & ADDRESS (if different from Controlling Office)

Air Force Technical Applications Center
VELA Seismological Center
Alexandria, Virginia 22314

15. SECURITY CLASS. (of this report)

UNCLASSIFIED

15a. DECLASSIFICATION/DOWNGRADING SCHEDULE

16. DISTRIBUTION STATEMENT (of this Report)

APPROVED FOR PUBLIC RELEASE, DISTRIBUTION UNLIMITED

17. DISTRIBUTION STATEMENT (of the abstract entered in Block 20, if different from Report)

18. SUPPLEMENTARY NOTES

ARPA Order No. 2551

19. KEY WORDS (Continue on reverse side if necessary and identify by block number)

Seismology	Discrimination	Polarization Filter
Signal Extraction	Bandpass Filter	Gaussian Narrow-band Filter
Cascaded Filters	Wiener Filter	
Detection	Chirp Matched Filter	

20. ABSTRACT (Continue on reverse side if necessary and identify by block number)

The purpose of this work was to develop and evaluate an interactive long-period signal extraction filter suite. Five filters were included in the suite and were applied to test data in a cascaded mode, (i.e., the output of one filter served as the input to the next filter). The filters tested were a bandpass filter, a Wiener filter, a chirp matched filter, a polarization filter, and a Gaussian narrowband

→over

DD FORM 1 JAN 73 1473 EDITION OF 1 NOV 65 IS OBSOLETE

UNCLASSIFIED

SECURITY CLASSIFICATION OF THIS PAGE (When Data Entered)

411669

JDB

20. (continued)

filter. It was found that, for the filters examined, the polarization filter dominates the cascaded filtering approach to signal extraction; specifically, processing gains as high as 14 to 15 dB were realized from the application of cascaded filters which included this filter. Further, tests performed on a Eurasian data set using one specific cascaded filter sequence yielded an improvement in surface wave detection capability equivalent to an improvement in bodywave detectability of approximately 0.6 to 0.8 m_b units. Finally, cascaded filters were found to provide more detected signals from which surface wave magnitudes can be obtained; as such, the use of these filters can enhance an analyst's capability to discriminate between earthquakes and explosions.

m sub b

This research was supported by the Advanced Research Projects Agency of the Department of Defense and was monitored by AFTAC/VSC, Patrick Air Force Base, FL 32925, under Contract Number F08606-79-C-0014.

AFTAC Project Number:	VELA T/9705/B/PMP
Project Title:	VELA Network and Automatic Processing Research
ARPA Order Number:	2551
Name of Contractor:	ENSCO, Inc.
Contract Number:	F08606-79-C-0014
Effective Date of Contract:	11 December 1978
Contract Expiration Date:	1 June 1980
Project Manager:	Theodore J. Cohen (703) 548-8666

SUMMARY

The purpose of this work was to develop and evaluate an interactive long-period signal extraction filter suite. Five filters were included in the suite and were applied to test data in a cascaded mode, (i.e., the output of one filter served as the input to the next filter). The filters tested were a bandpass filter, a Wiener filter, a chirp matched filter, a polarization filter, and a Gaussian narrowband filter. It was found that for the filters examined, the polarization filter dominates the cascaded filtering approach to signal extraction; specifically, processing gains as high as 14 to 15 dB were realized from the application of cascaded filters which included this filter. Further, tests performed on a Eurasian data set using one specific cascaded filter sequence yielded an improvement in surface wave detection capability equivalent to an improvement in bodywave detectability of approximately 0.6 to 0.8 m_b units. Finally, cascaded filters were found to provide more detected signals from which surface wave magnitudes can be obtained; as such, the use of these filters can enhance an analyst's capability to discriminate between earthquakes and explosions.

TABLE OF CONTENTS

TABLE OF CONTENTS
(continued)

LIST OF FIGURES

LIST OF TABLES

SECTION I
INTRODUCTION

A. THE TASK

This report presents the results of a study performed on cascaded, long-period signal extraction techniques. The purpose of the study was fourfold. First, it was desired to integrate a suite of long-period filters into an interactive seismic processing system. Second, the procedures for using the filters in a cascaded mode were to be standardized and optimized for automatic mode operation. Third, the filter program was to be tested for its effect on signal detection and event discrimination. Fourth, the feasibility and operability of using the long-period signal extraction program on a large, world-wide data base were to be determined.

Early in the course of the study, a problem arose which forced a change in the manner in which the work was performed. Specifically, the problem was that computation of a fast Fourier transform (FFT) on the PDP-15/50 (an interactive processing system) is significantly slower than it is on the IBM 360/44 (batch processing system). Since the polarization filter used here requires many FFTs in order to compute and apply the appropriate filter weights, the relatively slow computational speed of the interactive system rendered impractical the processing of large data bases.

To circumvent this problem, the interactive filter program was primarily used to estimate the optimum values of these filter parameters which had not been determined in earlier signal extraction studies (Strauss, 1978). The interactive system was also used to test the filter algorithms as each was designed. However, to perform tests of the cascaded filters on large data bases a similar filter program suite was developed for use on the batch processing system (hereafter referred to as the automatic mode of processing) using the optimum values of the controlling parameters which were determined by means of the interactive system.

It should be noted that the problem described above (the FFT computational speed on the PDP-15/50) is not common to all interactive systems. A transfer of the programs developed here to a system such as a PDP-11/70 with an array-processor subsystem would provide for efficient, interactive processing of large data bases. The transfer of the interactive signal extraction program to another system remains as a subject for future study.

B. SUMMARY OF PREVIOUS WORK

A number of studies have been made on the use of specific filtering techniques for long-period signal extraction. Relevant results obtained in some of these studies are summarized in Table I-1. In each case, the signal extraction technique was applied to 'raw' (i.e., previously unfiltered) data. Note that of the filters examined, the greatest improvement in the signal-to-noise ratio (SNR) was obtained using the polarization filter (7.5 dB to 10 dB for Rayleigh waves).

TABLE I-1

SUMMARY OF PREVIOUS SIGNAL EXTRACTION RESULTS
USING VARIOUS FILTERING TECHNIQUES

Extraction Technique	Processing Gain (dB)	Source Of Test Data	Reference
Chirp Matched Filter	3	Eurasian earthquakes recorded at a single site of the Alaskan Long Period Array	Strauss, 1973
Reference-Waveform Matched Filter	3		Strauss, 1973
Polarization Filter: Rayleigh Waves Love Waves	 7.5 6.5		Strauss, 1976
Wiener Filter	2-6	Kurile Islands - Kamchatka earthquakes recorded at the Guam Seismic Research Observatory	Lane, 1976
Bandpass Filter - Polarization Filter (Rayleigh Waves)	10		Lane, 1977
Wiener Filter - Polarization Filter (Rayleigh Waves)	10		Lane, 1977
Wiener Filter - Polarization Filter (Rayleigh Waves)- Reference-Waveform Matched Filter	8		Lane, 1977

The first results obtained using cascaded filters of the types discussed here (Lane, 1977) are also presented in Table I-1. Note that when a reference-waveform matched filter was cascaded with other extraction techniques it lowered the net gain of the cascaded filters by 2 dB. This result may be due to the difficulty encountered in selecting a suitable reference event from a complex source region such as the Kurile Islands. Based on this result, chirp matched filters were substituted for reference-waveform matched filters in the present study.

C. SPECIFIC GOALS

The specific goals of this study are to:

- Integrate available long-period, signal-extraction filtering programs into an interactive seismic processing system;
- Standardize and optimize the procedures for using the interactive seismic processing system;
- Create an automatic mode processing version of the interactive program;
- Estimate SNR improvement produced by the application of cascaded filtering techniques;
- Estimate the effects of cascaded filtering techniques on detection capability;
- Estimate the effects of cascaded filtering techniques on earthquake/explosion discrimination capability;

- Determine the feasiblity and operability of using the new long-period filtering program on a large, world-wide data base.

The work performed to fulfill each of these goals is presented as follows. Section II presents a description of each of the filtering techniques used and of the method used to combine these techniques into interactive and automatic mode programs. Also included in this section is a description of the controlling parameters peculiar to each filtering technique.

Section III presents information on the SNR improvement obtained from various sequences of cascaded filtering. A discussion of the optimum cascaded filter sequence is also presented.

Sections IV and V present the results of an experiment performed on a large data base using one specific sequence of cascaded filters. The results of the experiment illustrate the effects on signal detection and discrimination produced by cascade processing. Specifically, Section IV discusses the improvement obtained in the detectability of seismic signals recorded by single stations and by a small network of stations. Section V discusses the effect of the filter sequence examined on earthquake/explosion discrimination by means of the M_s-m_b discriminant.

Finally, Section VI summarizes the results of this study and, based on the results obtained, discusses the feasibility of using cascaded filters on a large, world-wide data base.

D. TEST DATA BASE

Test events used in studies such as this should be located in the same region in order to minimize the effects of source-receiver path differences on event detection and discrimination. Accordingly, approximately 200 earthquakes which occurred between August 1978, and April 1979, and which had epicenters in the Kashmir-Uzbek-Tadzhik area (as listed in the Norwegian Seismic Array event bulletin) were selected for the earthquake test data base. Since no region yielded an appreciable number of presumed explosions during the time frame noted above, all Eurasian presumed explosions were selected for use in the discrimination test. Data for all events were edited from the digital magnetic tapes recorded at the Ankara, Turkey (ANTO); Shillong, India (SHIO); Taipei, Taiwan (TATO); Matsushiro, Japan (MAJO); Guam, Marianas Islands (GUMO); Chiang Mai, Thailand (CHTO); Kongsberg, Norway (KONO); and Grafenburg, Germany (GRFO) Seismic Research Observatories. The source regions and recording stations are shown in Figure I-1, where a solid circle (●) represents a station, a star (*) represents a presumed nuclear explosion (PNE) source location, and the solid square (■) represents the earthquake source region. The PNE locations were taken from bulletins of the National Earthquake Information Service (NEIS).

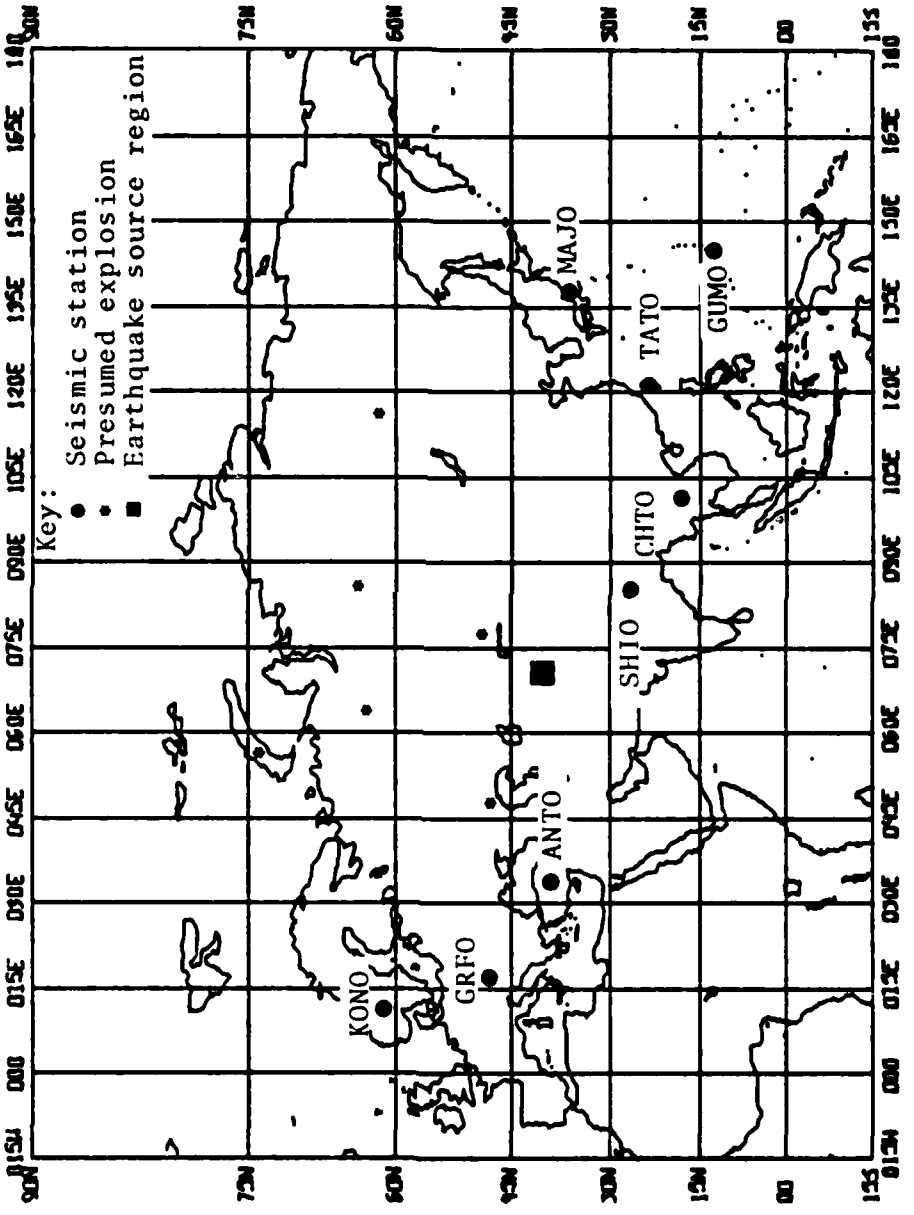

FIGURE I-1

LOCATIONS OF RECORDING STATIONS AND SOURCE REGIONS

SECTION II
THE LONG-PERIOD SIGNAL EXTRACTION PROGRAM

A. GENERALIZED STRUCTURE OF THE PROGRAM

The general structure of the long-period signal extraction program is shown in Figure II-1. Both the interactive and automatic mode versions can be considered to have four processing stages: (1) prepare and display data; (2) select filter; (3) apply filter; and (4) display filtered data and make magnitude measurements. Both versions were designed for ease of insertion of additional signal extraction algorithms. For the interactive program, this is accomplished through user functions (Shaub and Black, 1977) while for the automatic mode program, this is accomplished through the use of subroutines.

Because of the FFT time constraint discussed in Section I, the interactive system was used primarily to determine the optimum manner in which to apply the automatic mode version of the program. Thus, each processing stage of the interactive program shown in Figure II-1 requires analyst intervention in the form of time gate and filter parameter selection. The automatic mode version of the program, on the other hand, requires no such intervention. Processing time gates are selected on the basis of expected waveform arrival times while filter parameters are preset.

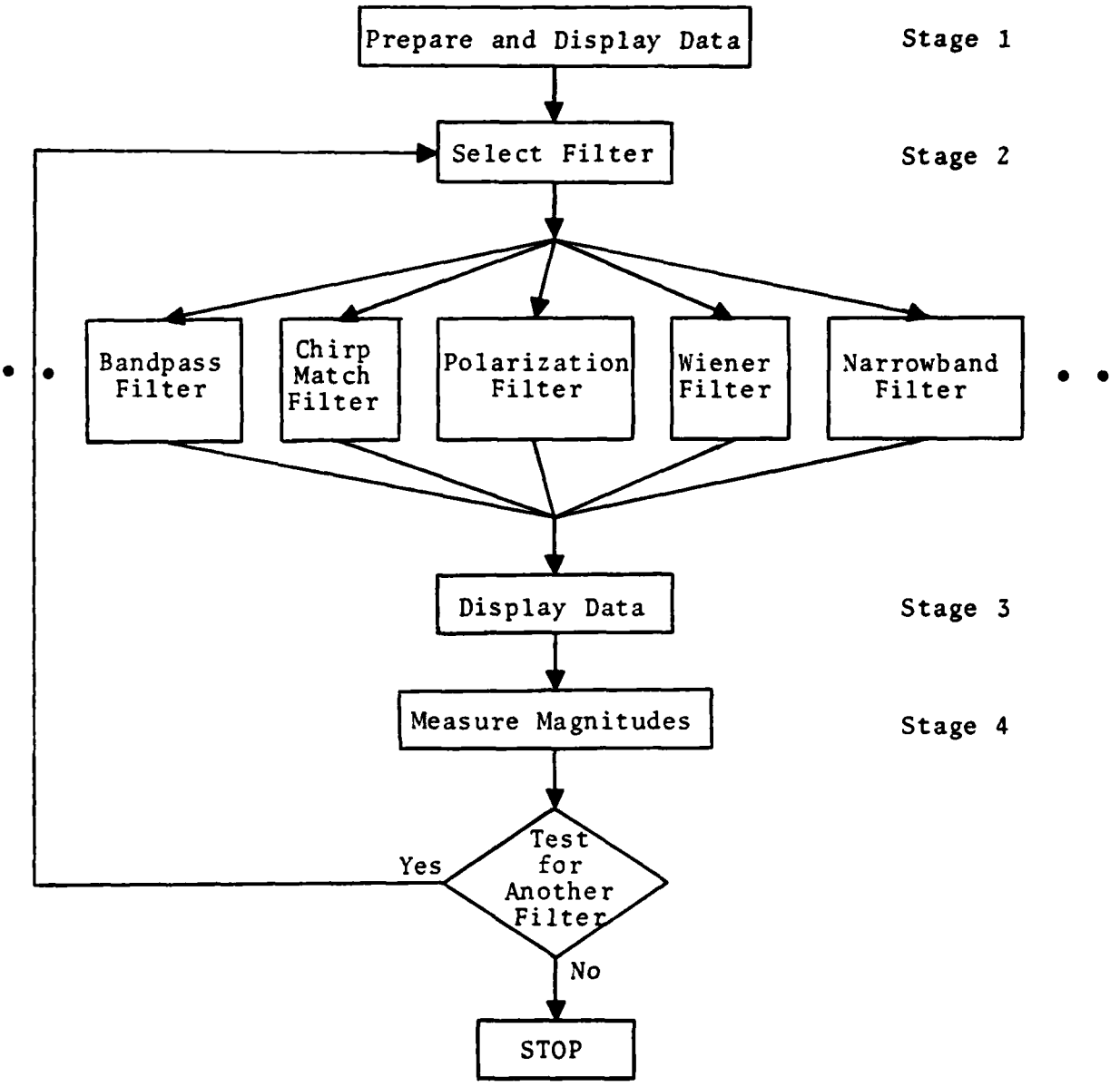

FIGURE II-1
PROGRAM STRUCTURE FOR CASCADED FILTERING

B. SIGNAL EXTRACTION TECHNIQUES

This section presents brief descriptions of the five filter techniques used in this study and the manner in which they are combined to form the long-period signal extraction program. The five filter techniques used are:

- Bandpass filter with cosine-squared taper
- Wiener filter
- Chirp matched filter
- Polarization filter
- Gaussian narrowband filter.

1. Bandpass Filter with Cosine-Squared Taper

The bandpass filter operates in the frequency domain, suppressing all power at frequencies below the low bandpass frequency (BPL) and above the high bandpass frequency (BPH) (see Figure II-2). The algorithm applies a cosine-squared taper to the power at those frequencies between BPL and BPL-plus-the-taper-length, and between BPH-minum-the-taper-length and BPH. (The taper, which is used to minimize filter ringing, was set to ten frequency points for this study.) The power at all remaining frequencies receives a filter weight of one (1.0).

The processing parameters which must be specified for this filter are the low and high bandpass cutoff frequencies, BPL and BPH, respectively. In general, these values were set at 0.023 Hz for BPL, and at 0.059 Hz for BPH; these values

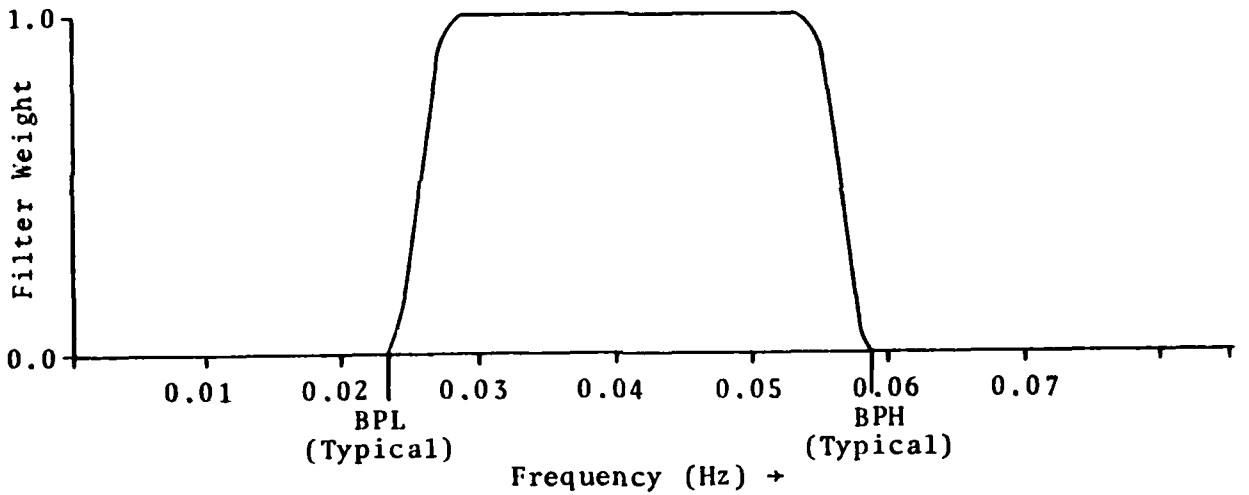

FIGURE II-2
FILTER WEIGHTS OF THE BANDPASS FILTER

roughly set the limits of the 'signal window' of the SRO noise spectra and exclude the microseismic noise peak at approximately 0.06-0.07 Hz (Strauss and Weltman, 1977). An exception to the use of these values for the bandpass cutoff frequencies will be noted in the discussion of chirp matched filters.

2. Wiener Filter

The Wiener filter used in this long-period signal extraction study is discussed by Lane (1976). Briefly, in the frequency domain, the Wiener filter takes the form

$$W(\omega) = \frac{\phi_{ss}(\omega)}{\phi_{ss}(\omega) + \phi_{nn}(\omega) + \phi_{sn}(\omega) + \phi_{ns}(\omega)}$$

where $W(\omega)$ are the filter weights, $\phi_{ss}(\omega)$ and $\phi_{nn}(\omega)$ are the autopower spectra of the signal and noise, respectively, and $\phi_{sn}(\omega)$ and $\phi_{ns}(\omega)$ are the crosspower spectra of the signal and noise.

It is generally assumed that the signal and noise are uncorrelated so that the terms $\phi_{sn}(\omega)$ and $\phi_{ns}(\omega)$ may be ignored. However, there may be some correlation, albeit small, between signal and noise due to the random nature of the noise. Attempts by Lane (1976) to calculate the signal-noise crosspower correlation terms, however, were not successful since the phase of the noise is a random variable. Although various models of the phase of the noise were examined for use with the Wiener filter, none was as effective as omitting

the correlation terms $\phi_{sn}(\omega)$ and $\phi_{ns}(\omega)$ entirely. The Wiener filter weights are, therefore, computed as follows:

$$W(\omega) = \frac{\phi_{ss}(\omega)}{\phi_{ss}(\omega) + \phi_{nn}(\omega)} \quad .$$

Two data items are necessary for the successful operation of this filter. First, a high SNR event from the source region under study is needed to compute the $\phi_{ss}(\omega)$ term. Second, a noise gate immediately preceding the test signal gate is required in order to compute the $\phi_{nn}(\omega)$ term. Lack of high SNR events or degraded noise data caused by instrument malfunctions will preclude use of this filter.

3. Linear Chirp Matched Filter

The signal extraction technique known as the linear chirp matched filter is, in essence, a cross-correlation operation of the form

$$\rho(t) = \int_{-\infty}^{\infty} g(\tau)\ f(t+\tau)\ d\tau$$

where $f(\tau)$ is the test time series and $g(\tau)$ is a synthetic dispersed waveform.

It is computationally easier to apply the chirp matched filter in the frequency domain since this requires only a series of multiplications rather than a numerical integration. To see this, first Fourier transform the above equation:

$$P(\omega) = \int_{-\infty}^{\infty} e^{-j\omega t} \left[\int_{-\infty}^{\infty} g(\tau)\ f(t+\tau)\, d\tau \right] dt \ .$$

Changing the order of integration:

$$P(\omega) = \int_{-\infty}^{\infty} g(\tau) \left[\int_{-\infty}^{\infty} e^{-j\omega t}\ f(t+\tau)\, dt \right] d\tau \ .$$

From the time-shifting theorem:

$$\int_{-\infty}^{\infty} e^{-j\omega t}\ f(t+\tau)\ dt \ = \ F(\omega)\ e^{j\omega\tau}$$

and so:

$$P(\omega) = \int_{-\infty}^{\infty} g(\tau)\ F(\omega)\ e^{j\omega\tau}\ d\tau = F(\omega) \int_{-\infty}^{\infty} g(\tau)\ e^{j\omega\tau}\ d\tau \ .$$

Now:

$$\left.\begin{aligned} G(\omega) &= \int_{-\infty}^{\infty} g(\tau)\ e^{-j\omega\tau}\ d\tau \\ G(-\omega) &= \int_{-\infty}^{\infty} g(\tau)\ e^{j\omega\tau}\ d\tau \end{aligned}\right\} \text{ by definition of the Fourier transform}$$

Therefore

$$P(\omega) = F(\omega)\ G(-\omega) \ .$$

Since

$$G(-\omega) = G^*(\omega), \quad \text{where } G^*(\omega) \text{ is the complex conjugate of } G(\omega),$$

$$P(\omega) = F(\omega)\ G^*(\omega).$$

The chirp matched filter response function $G(\omega)$ is defined by

$$G(\omega) = e^{j \frac{L\Delta t}{4(\omega_H - \omega_L)} (\omega - \omega_o)^2} \qquad \text{for } \omega_L \leq \omega \leq \omega_H$$

$$= 0 \qquad \text{otherwise}$$

and

$$G(-\omega) = G^*(\omega)$$

where

ω_L is the lowest frequency of the chirp matched filter

ω_H is the highest frequency of the chirp matched filter

ω_o is the frequency at which zero phase shift occurs

L is the length (in points) of the corresponding time-domain chirp matched filter

Δt is the sampling interval of the data, in seconds per sample.

The frequency domain response function corresponds to a dispersive time-domain waveform with a linear group delay and an essentially flat ampltiude at all frequencies in the band $\omega_L \leq \omega \leq \omega_H$ (Harley, 1971).

The processing parameters required for the operation of the chirp matched filter are the lowest and highest frequencies, and the length of the chirp waveform.

4. Polarization Filter

The polarization filter computes and applies filter weights in the frequency domain to three-component data which have been rotated to a vertical, transverse, radial configuration (see Strauss, 1979). The assignment of filter weights is based on the measured difference in phase between the radial and vertical components as compared to the expected difference in phase for a given mode of propagation. For Rayleigh waves, this expected phase difference is 90^{o}. The filter weights are assigned on a frequency-by-frequency basis using overlapping data segments; thus, the polarization filter adapts to time-varying signal and noise conditions.

A separate algorithm is invoked in parallel with the polarization filter to extract Love waves (see Strauss, 1979). Briefly, this algorithm determines, on a frequency-by-frequency basis, the difference between the expected arrival azimuth of the Love wave and the actual arrival azimuth. All energy with arrival azimuth differences outside some range about the expected Love wave arrival azimuth is rejected as noise. Like the Rayleigh wave polarization filter, the Love wave polarization filter is time-adaptive.

5. Gaussian Narrowband Filter

For the Gaussian filter, the filter weights form a Gaussian distribution with center frequency ω_o, and with half-amplitude bandwidth $\Delta\omega$ (see Figure II-3). The filter weights $H(\omega)$ are defined by:

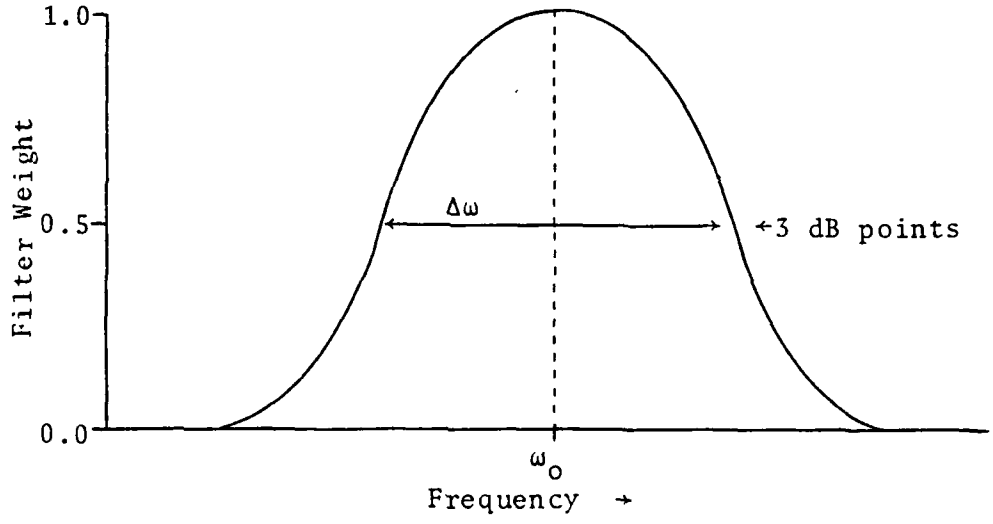

FIGURE II-3
FILTER WEIGHTS OF GAUSSIAN NARROWBAND FILTER

$$H(\omega) = \beta\left[e^{\frac{(\omega-\omega_o)^2}{-2\sigma^2}} + e^{\frac{(\omega+\omega_o)^2}{-2\sigma^2}}\right]$$

where:

ω_o = center frequency of the filter

β = gain parameter; $\beta \simeq 1$ to provide unit gain at ω_o

σ^2 = bandwidth parameter related to the 3 dB down points by:

$$H(\omega_o + \Delta\omega) \simeq 0.5\, H(\omega_o) = 0.5\beta \ ;$$

thus,

$$0.5\beta \simeq \beta\left[e^{\frac{(\omega_o + \Delta\omega/2) - \omega_o^2)^2}{-2\sigma^2}}\right]$$

$$\ell n(0.5) \simeq \frac{(\omega_o + \Delta\omega/2) - \omega_o)^2}{-2\sigma^2} = -\frac{(\Delta\omega)^2}{8\sigma^2}$$

and

$$\sigma^2 \simeq -\frac{(\Delta\omega)^2}{8\ell n(0.5)} \ .$$

Thus, the Gaussian narrowband filter requires two processing parameters: the center frequency ω_o, and the half-amplitude bandwidth $\Delta\omega$.

C. THE INTERACTIVE SIGNAL EXTRACTION PROGRAM

Implementation of the interactive long-period signal extraction program was based on the Extended Interactive Seismic Processing System (ISPSE) originally formulated by

Ringdal, Shaub, and Black (1975), and improved by Shaub and Black (1977). For this study, ISPSE provides the analyst with two system functions and with the ability to create new user functions as needed. The first system function, SELEV, permits the analyst to retrieve a desired waveform from a disk, to display the waveform, and to select a processing time gate. (The data on the disk are obtained from a magnetic tape containing waveforms which were previously edited and rotated to a vertical, transverse, radial orientation.) The second system function, FILTER, permits the analyst to apply bandpass filters and chirp matched filters to the data; to measure RMS noise, peak amplitude, and surface wave magnitude; and to display the data after each operation. Thus, FILTER contains two of the five filters shown in Figure II-1, and post-filtering display and magnitude measurement capabilities.

To complete the interactive program, three user functions (analogous to subroutines) were created. These are POLAR, the polarization filter algorithm, GAUSS, the Gaussian narrowband filter, and WIEN, the Wiener filter. These user functions may be applied at the analyst's discretion at any point after the processing time gate has been selected by means of SELEV. To display the filtered data and to make any measurements desired, the analyst returns to FILTER following execution of the user function.

An example of the application of the interactive signal extraction program is shown in Figure II-4. To produce this figure, the following steps were taken:

- SELEV - analyst selected event to process and the processing time gate
- FILTER - analyst displayed raw data and measured SNR values
- POLAR - analyst applied polarization filter
- FILTER - analyst displayed polarization filtered data and measured SNR values
  - analyst applied chirp matched filter to polarization filtered data
  - analyst displayed polarization, chirp matched filtered data and measured SNR values.

An example of the application of the interactive program to the problem of filter parameter optimization is shown in Figure II-5. The parameter to be optimized is the length of the chirp matched filter. (The sample rate for all data is one sample every two seconds.) The top trace of Figure II-5 shows the vertical component of the Rayleigh wave which was generated by a Eurasian event and which was recorded at ANTO. The initial and final frequencies of the chirp matched filter were set at 0.024 and 0.077 Hz, respectively. In the example shown, chirp filters with lengths of 140, 190, 240, and 290 points were successively applied to the data shown at the top trace, and the results were displayed as shown. The bottom trace shows the 240-point chirp filter. By means of the parameter measurement module of FILTER, the SNR values of the traces were then measured. These results show that a chirp filter length of 240 points produces the best results for this waveform in the sense that this filter length maximizes the SNR.

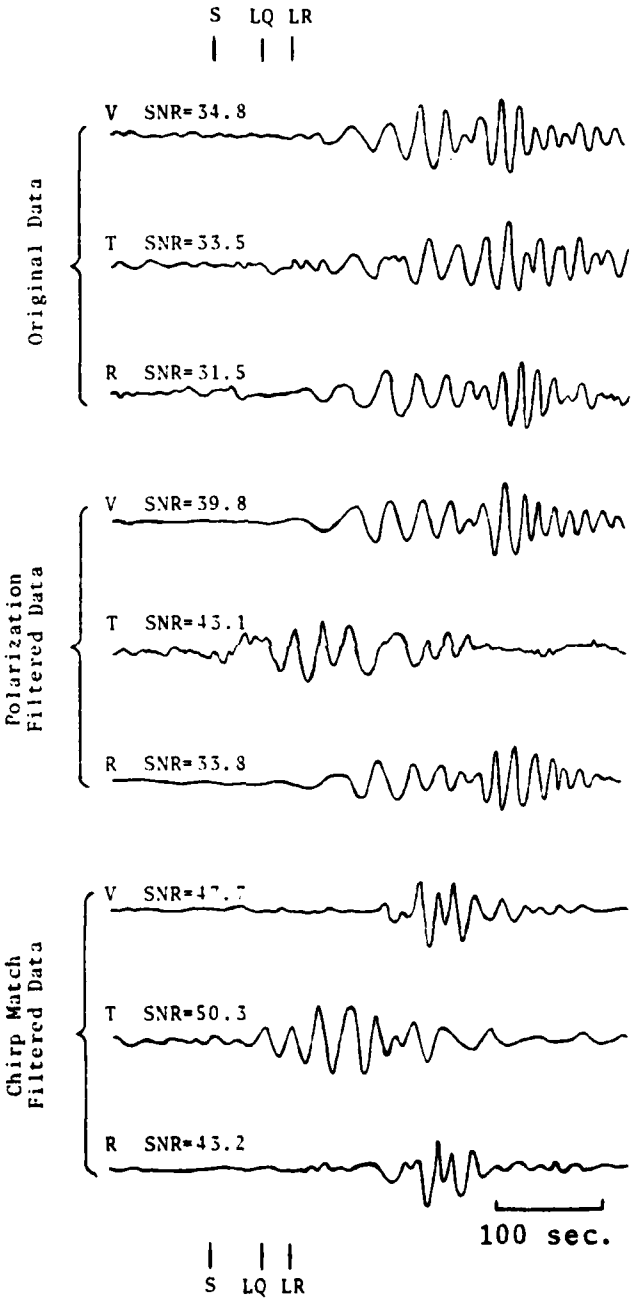

FIGURE II-4

EXAMPLE OF INTERACTIVE CASCADED FILTERING

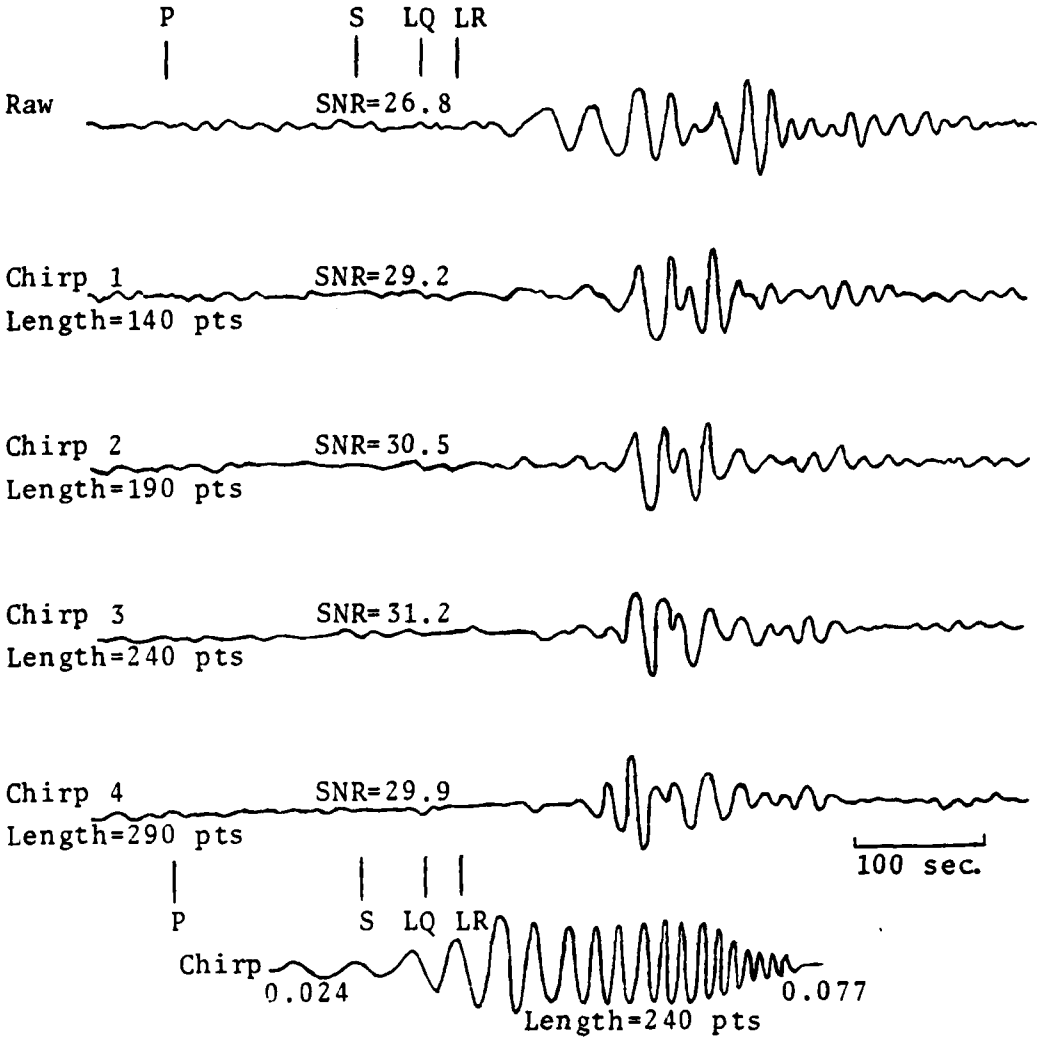

FIGURE II-5
OPTIMIZATION OF CHIRP MATCHED FILTER LENGTH

Processing a suite of test events in the manner described above produced the optimum chirp filter lengths listed in Table II-1 for data recorded at ANTO. The subregion numbers used in this table are those defined by Flinn and Engdahl (1965). The change in chirp filter length from subregion to subregion indicates the necessity of making this type of filter parameter evaluation whenever data from a new station-source region combination are to be processed.

In the past, attempts have been made to determine a linear relationship between the length of the synthetic chirp filter and the epicentral distance (Δ) of the test event. For example, Strauss and Tolstoy (1974) derived the following relationship:

$$\text{CHIRP FILTER LENGTH} = 10.27 * \Delta - 159.$$

However, the variance of the observed data about the data predicted by this relationship was too large to permit a credible determination of chirp filter length using epicentral distance.

Table II-1 also presents the results of testing for optimum chirp filter length using data previously processed by the polarization filter. Note that in general, the optimum chirp filter lengths determined for polarization-filtered data are shorter than the optimum chirp filter lengths determined for raw data. This illustrates that care must be taken in setting the processing parameters for each stage of a cascaded filter sequence since a parameter which is optimum for one filter sequence is not necessarily optimum for another.

TABLE II-1

OPTIMUM CHIRP MATCHED FILTER LENGTH FOR DATA FROM SELECTED SEISMIC SUBREGIONS AS RECORDED AT ANKARA, TURKEY (ANTO)

Flinn and Engdahl (1965) Subregion	Optimum Chirp Filter Length In Points			
	Chirp Filter Applied To Raw Data		Chirp Filter Applied To Polarization Filtered Data	
	Rayleigh	Love	Rayleigh	Love
336	240	260	220	260
716	360	300	600	500
711	480	400	480	260
648	260	300	240	240
329	690	660	670	600
302	345	335	380	300

D. THE AUTOMATIC MODE SIGNAL EXTRACTION PROGRAM

The automatic mode signal extraction program is structured as shown in Figure II-1. In its present state, the program requires, as input, 2048-point waveform edits of three-component, rotated data. Based on experience gained using the individual filters and the interactive signal extraction program, the processing parameters of the various filter algorithms can be set as follows:

- Two passbands are sufficient to prefilter the data. If a chirp matched filter is included in the cascaded filtering sequence, the passband is set at 0.020-0.080 Hz in order to avoid eliminating frequencies used by the chirp matched filter. If the chirp matched filter is not included in the filtering sequence, the passband is set at 0.023-0.059 Hz.
- The key input data item for the operation of the Wiener filter is the high SNR waveform required to compute $\phi_{ss}(\omega)$. The data are obtained from a magnetic tape which contains signals with high SNRs from each source region of interest.
- The initial and final frequencies of the chirp matched filter are set at 0.024 Hz and 0.077 Hz, respectively. These frequency values were determined from a study of the dispersion of signals recorded at ANTO. The length of the chirp matched filter is determined from Table II-1.
- The polarization filter requires two parameters to be preset. These are the number of points per processing segment and the width of the pass window

used in computing the filter weights. Optimum values of these parameters, determined by Lane (1976) for long-period surface waves, were used in the automatic mode version of signal extraction program.

- The Gaussian narrowband filter requires two parameters to be preset. These are the center frequency and the half-amplitude width of the filter. The center frequency is determined by the program by computing a smoothed power spectrum of the data in the signal gate and then finding the frequency at which the spectrum has its maximum value. This frequency is used as the center frequency of the filter. The half-amplitude width of the filter is set to one-half the center frequency.

It is seen from the above that the automatic mode version of the cascade filter program requires minimal input from the analyst. For example, the bandpass filter/polarization filter/Gaussian narrowband filter cascaded filter sequence (which is used extensively in Sections IV and V) requires only the designation of the signal to be analyzed since the filter parameters are either preset and remain constant, or are determined from the data itself.

SECTION III

ESTIMATION OF SIGNAL-TO-NOISE RATIO IMPROVEMENT PRODUCED BY THE APPLICATION OF CASCADED FILTERS

The approach used to estimate SNR improvement produced by various cascade filter sequences was to (1) process a suite of test events with various cascaded filter sequences; (2) determine the SNR gain for each test event and filter used; and (3) compute the mean SNR gain obtained using each filter sequence. The test data selected consisted of recordings for ten earthquakes which were located in the source region shown in Figure I-1, and recordings from seven presumed explosions (two from eastern Kazakh, two from the Ural mountains area, one from southwestern Russia, one from Novaya Zemlya, and one from central Siberia). All data were recorded at the Ankara, Turkey, (ANTO) Seismic Research Observatory.

Not all possible combinations of the five filters in the signal extraction program were used in this test since some combinations are 'illegal' (illegal combinations are those for which application of one filter destroys the signal characteristic upon which the operation of a subsequent filter depends). For example, the narrowband filter cannot be followed by the chirp matched filter or by the Wiener filter since the latter two filters use the dispersion characteristic of the signal which is eliminated by the narrowband filter.

The bandpass and Wiener filters were used to prefilter the data; their primary value was seen to be to cleanse the data by suppressing the noise while minimally affecting the signal. Using these filters first insured that data provided to succeeding filters were in the best possible form. The Gaussian narrowband filter, on the other hand, was used (with one exception where it was used as a pre-filter to the polarization filter) as a post-filter to reject all energy except that of the dominant frequency in the signal gate.

Table III-1 presents the results of this SNR gain improvement test. The letter codes in the column headed 'Cascaded Filter Combination' are defined as follows:

- B_1 - 0.023-0.059 Hz bandpass filter
- B_2 - 0.020-0.080 Hz bandpass filter
- W - Wiener filter
- C - Chirp matched filter
- P - Polarization filter
- G - Gaussian narrowband filter.

The order of the letters in each code indicates the order in which the filters were applied. The SNR gains of the individual filters over the raw data are also presented for purposes of comparison. Note that the Love wave gains were determined only from earthquake test events since explosion-generated Love waves are difficult to detect.

It is clear from the data of Table III-1 that the polarization filter dominates the signal extraction process. In fact, the gain of this filter alone is greater than that of

TABLE III-1

SNR GAINS PRODUCED BY VARIOUS CASCADED FILTER SEQUENCES

Cascaded Filter Sequence	LR-V SNR Gain		LQ-T SNR Gain	
	Mean (dB)	Standard Deviation (dB)	Mean (dB)	Standard Deviation (dB)
B_1	2.3	1.3	3.2	1.8
B_2	0.3	0.5	1.1	1.3
W	3.7	2.3	4.2	2.6
C	3.4	1.7	2.6	2.5
P	10.5	3.3	4.5	2.7
G	3.8	2.1	4.6	2.6
B_1, P	11.4	3.0	4.9	3.8
B_1, G	3.9	1.9	5.7	1.8
B_2, C	3.4	1.7	2.6	2.5
W, C	4.7	2.5	5.0	2.7
W, P	13.2	4.2	7.5	7.0
G, P	13.6	3.7	5.2	4.2
B_1, P, G	13.9	3.4	6.3	4.3
B_2, C, P	12.3	3.6	3.0	4.6
B_2, C, G	5.0	1.9	3.4	4.3
B_2, P, C	12.2	3.6	2.4	4.0
W, C, P	13.2	5.1	7.7	4.1
W, C, G	4.4	2.8	5.8	3.2
W, P, C	13.3	4.7	3.9	7.7
W, P, G	14.8	4.7	7.7	6.1
B_2, C, P, G	14.3	4.3	5.6	4.1
B_2, P, C, G	14.2	4.2	3.5	5.5
W, C, P, G	14.9	5.4	8.0	5.7
W, P, C, G	14.9	5.7	2.4	6.8

any of the cascaded filter sequences which does not include it. This is not to say, however, that those cascaded filter sequences which do not contain the polarization filter should be disregarded. It must be remembered that the polarization filter requires three-component, rotated (vertical, transverse, radial) data for successful operation. Thus, should the data be unrotated or should data for only one component (vertical) be available, it will not be possible to use any cascade filter sequence containing the polarization filter.

In almost all cases shown in Table III-1, replacement of the bandpass filter by the Wiener filter produces higher SNR gains. This increase in gain, however, is counterbalanced by the Wiener filter's need for a high SNR signal and a noise gate preceding the signal arrival of the test event in order to compute the filter weights. This raises the point that some cascaded filter sequences may be difficult to apply in an automatic mode of operation since they depend on the availability of information external to the test data.

Although cascading a series of filters produces higher mean SNR gains, the individual filter gains are not strictly additive. This is illustrated by Table III-2, which is derived from the data of Table III-1. In Table III-2, the 'expected gain' is the sum of the appropriate individual filter gains listed in Table III-1, while the 'actual gain' is the gain computed from applying the cascaded filter sequence. The letter codes have the same meaning as in Table III-1. This is only one of many examples which may be drawn from Table III-1. The point is that adding more filters to the cascaded filter sequence should not be expected to increase

TABLE III-2

COMPARISON OF ACTUAL AND EXPECTED GAINS
OF CASCADED FILTERS

Cascaded Filter Stage	Expected Gain	Actual Gain
B_2	0.3	0.3
B_2, C	3.7	3.4
B_2, C, P	14.2	12.3
B_2, C, P, G	18.0	14.3

substantially the SNR gain of the sequence. In general, it would appear that the most efficient cascaded filter sequence is a three-stage filter.

Based on the improvement in SNR gain, on the degree of variance in the gain, and on the ease of application to a large, world-wide data base using the automatic mode of operation, the favored cascaded filter sequence is the bandpass filter/polarization filter/Gaussian narrowband filter sequence (B_1, P, G of Table III-1). This sequence is used in Sections IV and V to illustrate the effects of cascaded filtering on detection and discrimination.

In order to estimate the stability of cascaded filter SNR gains for different source-receiver paths, the bandpass filter/polarization filter/Gaussian narrowband filter sequence was tested on earthquake-generated surface waves recorded at each of the stations shown in Figure I-1. The results of this test are summarized in Table III-3 in terms of the degree of RMS noise suppression, the degree of peak signal suppression, and the resulting gain in SNR. These results show that the SNR gain varies significantly from station to station. This suggests that the cascaded filter sequence which yields optimum results when applied to data recorded at one station may not be the best sequence to apply to data recorded at other stations. One reason for this may be that the noise at different stations exhibits significantly different characteristics, and these effects should be taken into account.

TABLE III-3

EFFECTS OF CASCADED BANDPASS FILTER/POLARIZATION FILTER/ GAUSSIAN NARROWBAND FILTER SEQUENCE ON DATA RECORDED AT NETWORK STATIONS

Station	Noise Suppression		Signal Suppression		Net Gain	
	Mean (dB)	Standard Deviation (dB)	Mean (dB)	Standard Deviation (dB)	Mean (dB)	Standard Deviation (dB)
ANTO	20.6	3.4	7.0	2.3	13.6	3.4
GUMO	27.3	6.9	12.1	5.9	15.2	7.6
GRFO	26.4	4.8	4.9	2.4	21.5	5.5
SHIO	23.0	5.4	5.6	2.9	17.4	3.8
TATO	23.0	4.5	8.2	3.0	14.8	3.5
MAJO	26.8	4.7	9.9	4.9	16.9	7.1
KONO	23.7	5.3	6.0	2.0	17.7	5.0
CHTO	23.7	2.8	7.3	3.6	16.4	5.3

SECTION IV
DETECTION CAPABILITY

A. SINGLE STATION TEST

This section describes the effects on single station and network detection capabilities produced by the application of a particular sequence of cascaded filters. This sequence consists of a 0.023-0.059 Hz bandpass filter, the polarization filter (using the Rayleigh and Love wave models), and the Gaussian narrowband filter (sequence B_1, P, G of Table III-1). This sequence is hereafter referred to as 'the cascaded filter.' This filter was selected on the basis of the SNR gain produced by its application and for its relative ease of application (the only input needed was the designation of each test event).

Two stations were selected to illustrate the single-station case: Ankara, Turkey (ANTO); and Kongsberg, Norway (KONO). The data base described in Section I served as the source of events, and consisted of 143 events recorded at ANTO and 139 events recorded at KONO. No presumed explosions were included in the data set since explosions exhibit a different surface wave detectability than do earthquakes. Furthermore, no events for which the data appeared to be mixed or showed low data quality (i.e., contained spikes or 'glitches') were included since such data tend to bias adversely the detection thresholds.

In short, the test described below is simply intended to demonstrate the improvement in event detectability produced by the selected cascade filter sequence. All of the detection capability estimates presented may be considered to be 'ideal' estimates in that it is implicitly assumed in their computation that the analyst will always see either seismic noise or the sought-after signal. That is, degraded data have been eliminated so that the analyst is working with an 'ideal' data set.

The data were first examined in their raw (unfiltered) form for visually detectable signals to provide a detection baseline against which the cascade filtered results could be compared. Each event was judged to be either 'detected' or 'non-detected', on the basis of whether the data showed signal-like characteristics (i.e., whether the data displayed the presence of dispersion in the signal gate, and whether the amplitudes in this gate were above those of the preceding noise gate). The number of detected and non-detected events for each bodywave magnitude were compiled, and the detection percentage was computed. Finally, a cumulative Gaussian distribution was fitted in a maximum likelihood sense (Ringdal, 1974) to these detection statistics.

After determining the detection status for the data in their raw form, the cascaded filter was applied to the data for each event. The data were plotted after each stage of the cascaded filter process in order to permit the analyst to determine the cumulative effect of each filter on the data. Detection capability curves of the type described above were then computed for each stage of the cascaded filter process.

The statistic used to judge the degree of improvement in the detection capability is the 50-percent detection threshold, m_{b50}. This is the bodywave magnitude at which the probability of detecting the associated surface waves is 50 percent. The analysis results are summarized in Table IV-1. The overall improvement in detection capability over that of the raw data produced by the cascaded filter sequence is approximately 0.8 m_b units for Rayleigh waves and 0.6-0.7 m_b units for Love waves.

One apparent anomaly in Table IV-1, however, is the approximately 0.2 m_b units improvement produced by the application of the bandpass filter to KONO data. One would expect improvements of perhaps 0.05-0.10 m_b units at this stage (as indeed is the case for the ANTO data) in light of the SNR improvement estimated for the bandpass filter in Section III. Reference to Figure IV-1, however, resolves this apparent anomaly. This figure, modified from data presented by Weltman, et al. (1979), shows the vertical component noise spectra for KONO and ANTO. As is seen, the microseismic peak of the noise at KONO is much higher than that at ANTO. Thus, application of the bandpass filter used here, which rejects the frequencies of the microseismic peak at KONO, will produce higher SNR gains at KONO than at ANTO. Had an interactive system be used, of course, the lower limit of the bandpass filter could easily have been revised to reject the microseismic peak at ANTO.

TABLE IV-1

DETECTION CAPABILITY IMPROVEMENT PRODUCED BY THE APPLICATION OF THE CASCADED FILTER - SINGLE STATION TEST

Data Type	50 Percent Detection Threshold (Bodywave Magnitude)			
	ANTO		KONO	
	LR-V	LQ-T	LR-V	LQ-T
Raw	4.77	4.80	4.62	4.75
Bandpass Filtered	4.72	4.75	4.43	4.57
Polarization Filtered	4.12	4.34	3.93	4.22
Narrowband Filtered	3.99	4.20	3.87	4.05

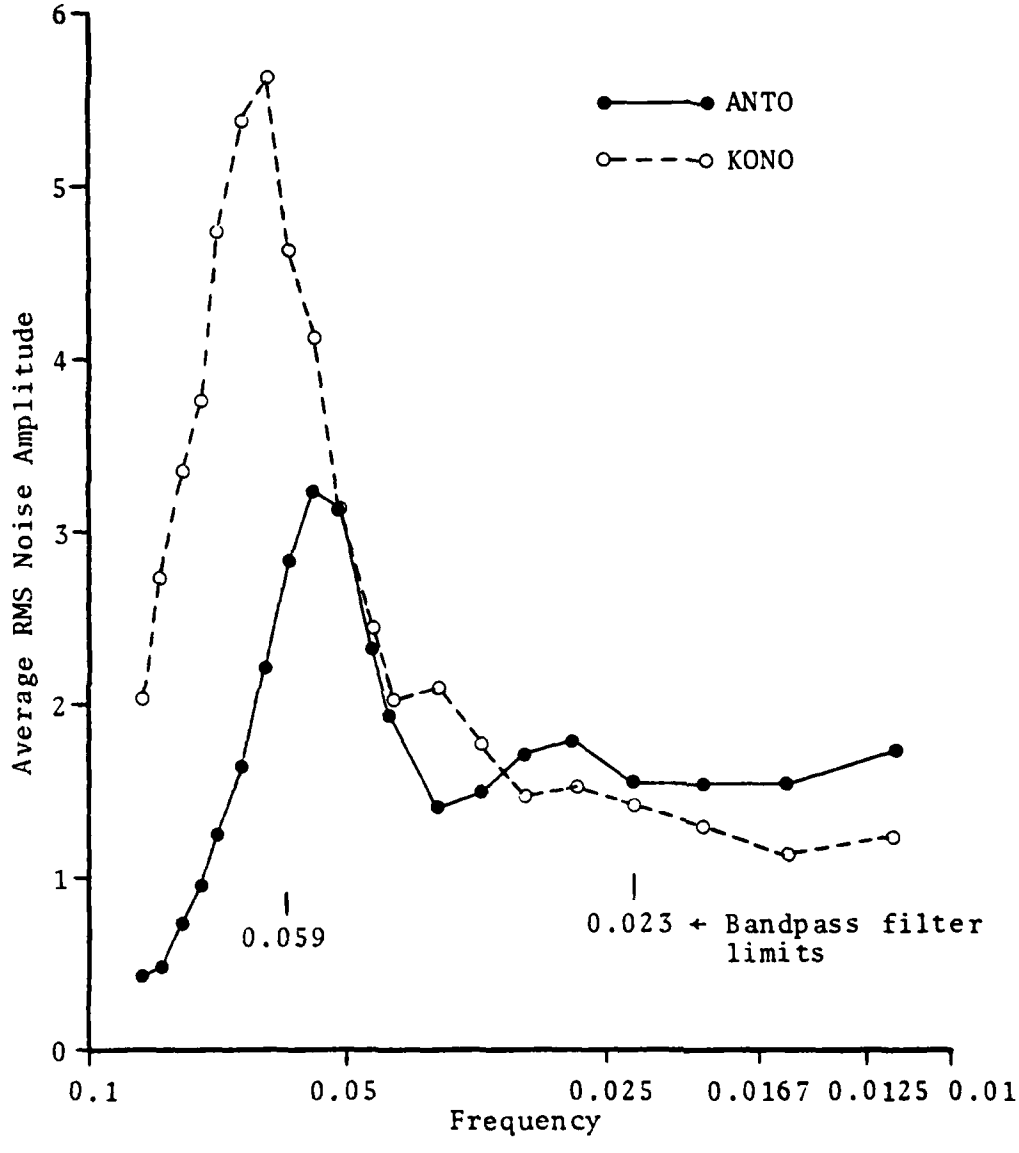

FIGURE IV-1
VERTICAL COMPONENT NOISE SPECTRA FOR ANTO AND KONO

B. NETWORK TEST

The approach taken to estimate the effects of the cascaded filter on network detection capability uses a modified version of the network capability estimation technique reported by Snell (1976). This technique is based on an analysis of the geometric mean noise amplitudes measured at the stations of the network (see Table IV-2). The signal amplitude at each of the network stations is calculated for an assumed event at epicenter j with bodywave magnitude m_{bj} (Equation IV-1). With signal and noise amplitudes assumed to be lognormally distributed, the probability that the SNR exceeds the individual station detection threshold is given by the normal cumulative probability function (Equations IV-2 and IV-3). The individual station detection probabilities are then combined into the network detection probability of at least α station detections, $\hat{P}_j(>\alpha)$, using a recursive relationship involving the individual station detection probabilities (Equation IV-4). A detailed description of this technique is given by Snell (1976). This technique was modified so that instead of computing detection threshold magnitudes for the network, the probability of detecting the surface waves of an event of given bodywave magnitude is plotted.

The geometric mean zero-to-peak noise amplitudes for bandpass filtered data were taken from the SRO evaluation report (Weltman, et al., 1979). To obtain the corresponding values for cascade filtered data, these values were reduced by factors determined from the mean filter gains of Table III-2.

TABLE IV-2

COMPUTATION OF NETWORK DETECTION CAPABILITY

$$\log_{10}(A_{ij}) = m_j + b_\Delta + c_\Delta * \log_{10}(\Delta_{ij}) + E_{ij} \quad \text{(IV-1)}$$

$$P_{ij} = \phi \frac{\log_{10}(A_{ij}) - (\mu_N + \log_{10}(SDT))}{(\sigma_n^2 + \sigma_s^2)^{\frac{1}{2}}} \quad \text{(IV-2)}$$

$$\phi(x) = \frac{1}{\sqrt{2\pi}} \int_{\infty}^{x} e^{-y^2/2}\, dy \quad \text{(IV-3)}$$

$$\hat{P}_j(\geq\alpha) = \sum_{k=\alpha}^{N} \hat{P}_j(k) \quad \text{(IV-4)}$$

where:

A_{ij}	-	Zero-to-peak signal amplitude at station i for event j
m_j	-	Bodywave magnitude of event j
b_Δ, c_Δ	-	Standard table entries
E_{ij}	-	Station-epicenter bias correction
μ_N	-	Geometric mean zero-to-peak noise amplitude
σ_n^2	-	Variance of $\log_{10}$ noise
σ_s^2	-	Variance of $\log_{10}$ signal
$\phi(x)$	-	Normal cumulative probability function
N	-	Number of stations in the network
$\hat{P}_j(k)$	-	Probability that k stations will detect event j
$\hat{P}_j(\geq\alpha)$	-	Probability that α or more stations will detect event j
SDT	-	Station detection threshold, i.e., signal-to-noise ratio required for detection at a station.

Using the methods described above, detection probabilities for an m_b=4.0 event with world-wide distribution of epicenters were computed in two ways: first, with the noise statistics computed from bandpass filtered data, and second, with the nosie statistics computed from cascade filtered data. Figure IV-2 shows the 0.5 probability-of-detection contours for these two cases. The dashed lines show the 0.5 probability-of-detection contour derived from bandpass filtered data, while the solid line shows the 0.5 probability-of-detection contour derived from cascade filtered data. The solid circles (•) denote the locations of the network stations. The shift of the 0.5 probability-of-detection contour away from the network illustrates the effect of cascade filtering on network event detectability.

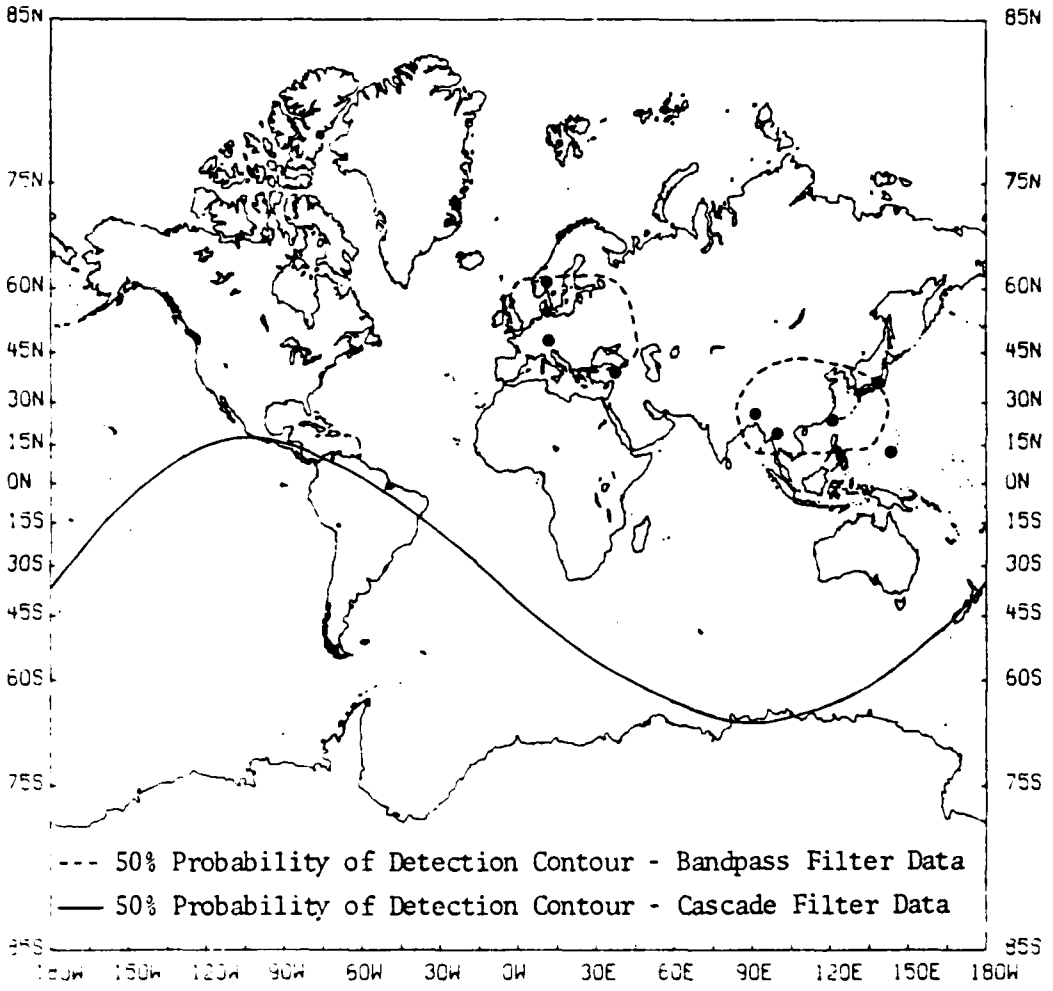

FIGURE IV-2

EFFECT OF CASCADED FILTERS ON NETWORK DETECTION CAPABILITY WHERE AT LEAST TWO STATION DETECTIONS ARE REQUIRED FOR NETWORK DETECTION OF AN m_b=4.0 EVENT

SECTION V
DISCRIMINATION CAPABILITY

A. SIGNAL MEASURABILITY

The previous section discussed the effects on detection capability of the bandpass filter/polarization filter/Gaussian narrowband filter cascaded filter sequence in terms of single station and network detection capabilities. This section considers the measurability of signals detected after such processing. The importance of examining signal measurability is that the increased detection capability of a station or network is of little value unless reliable magnitudes can be measured from the newly detected signals.

The first step in assessing the impact of cascaded filtering on the earthquake/explosion discrimination problem using the M_s-m_b discriminant involves measuring surface wave magnitudes for those events which were detected after bandpass filtering as well as after cascaded filtering using the bandpass filter/polarization filter/Gaussian narrowband filter sequence. These pairs of M_s values were then plotted as shown in Figure V-1 for the ANTO data, in Figure V-2 for the KONO data, and in Figure V-3 for the network data (where the network is the same as described in Section IV). A least-mean-square-error fit was subsequently made to each data set, as shown in these figures.

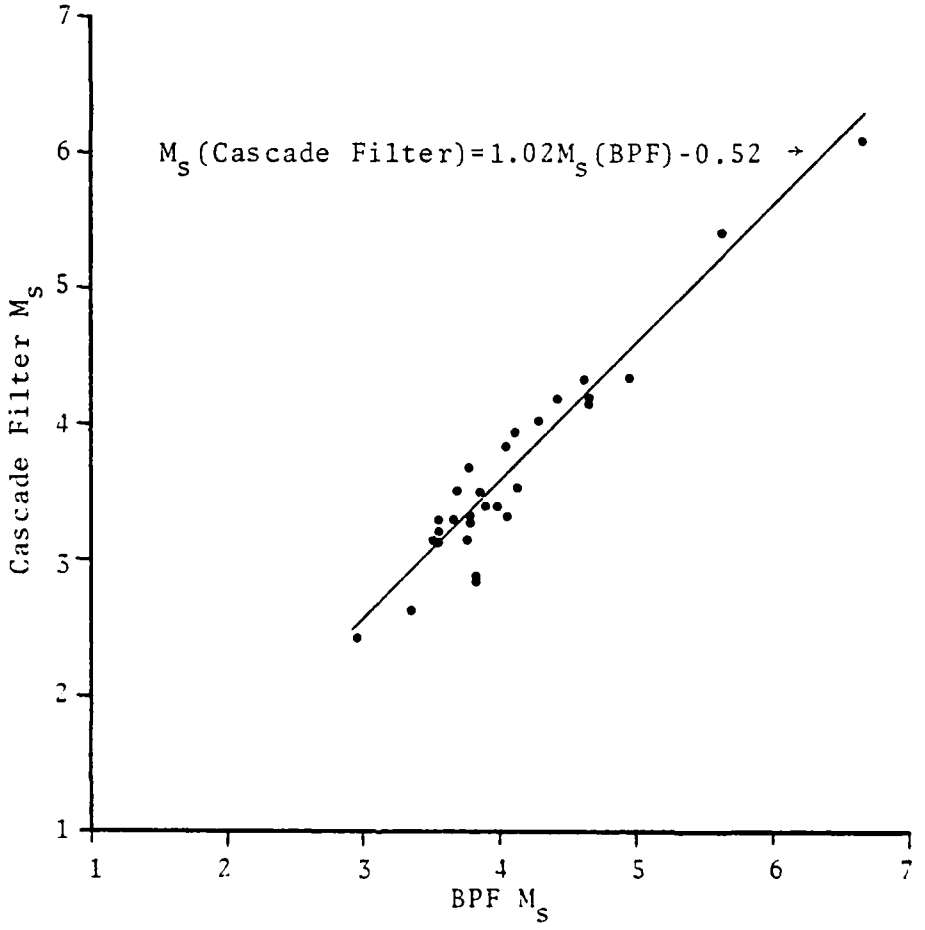

FIGURE V-1

COMPARISON OF M_S MEASURED ON BANDPASS FILTERED DATA TO M_S MEASURED ON CASCADED FILTERED DATA (ANTO)

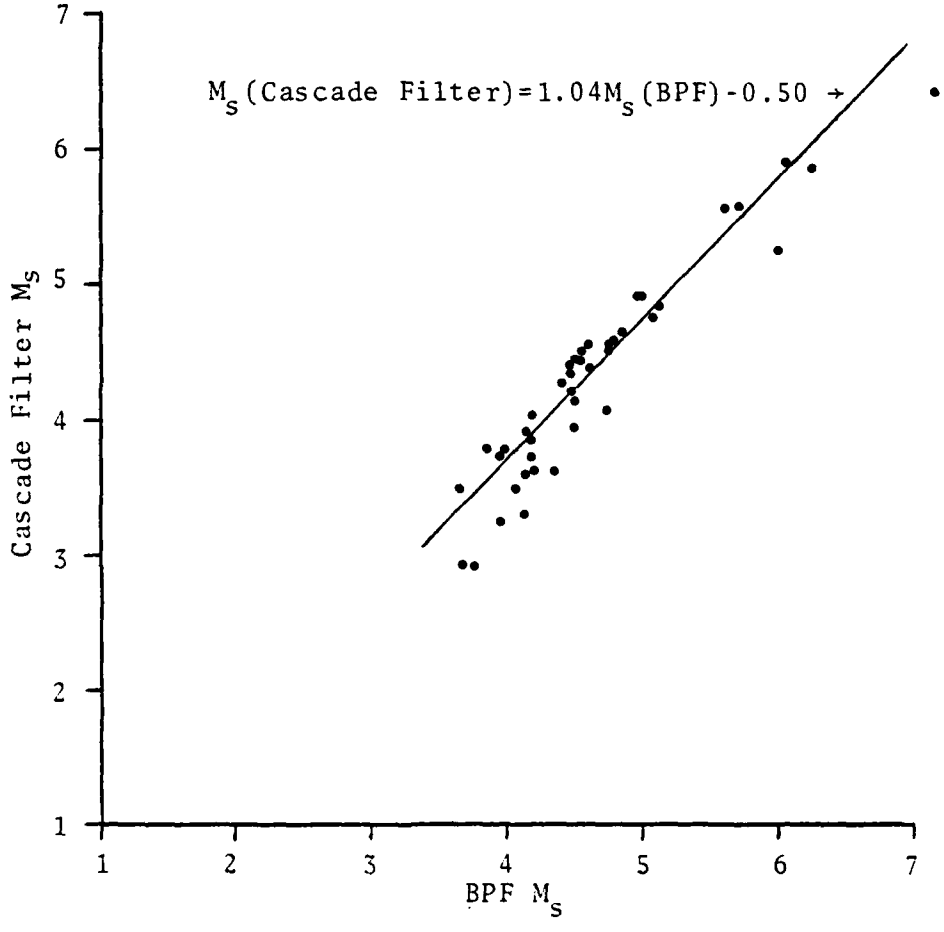

FIGURE V-2

COMPARISON OF M_s MEASURED ON BANDPASS FILTERED DATA TO M_s MEASURED ON CASCADED FILTERED DATA (KONO)

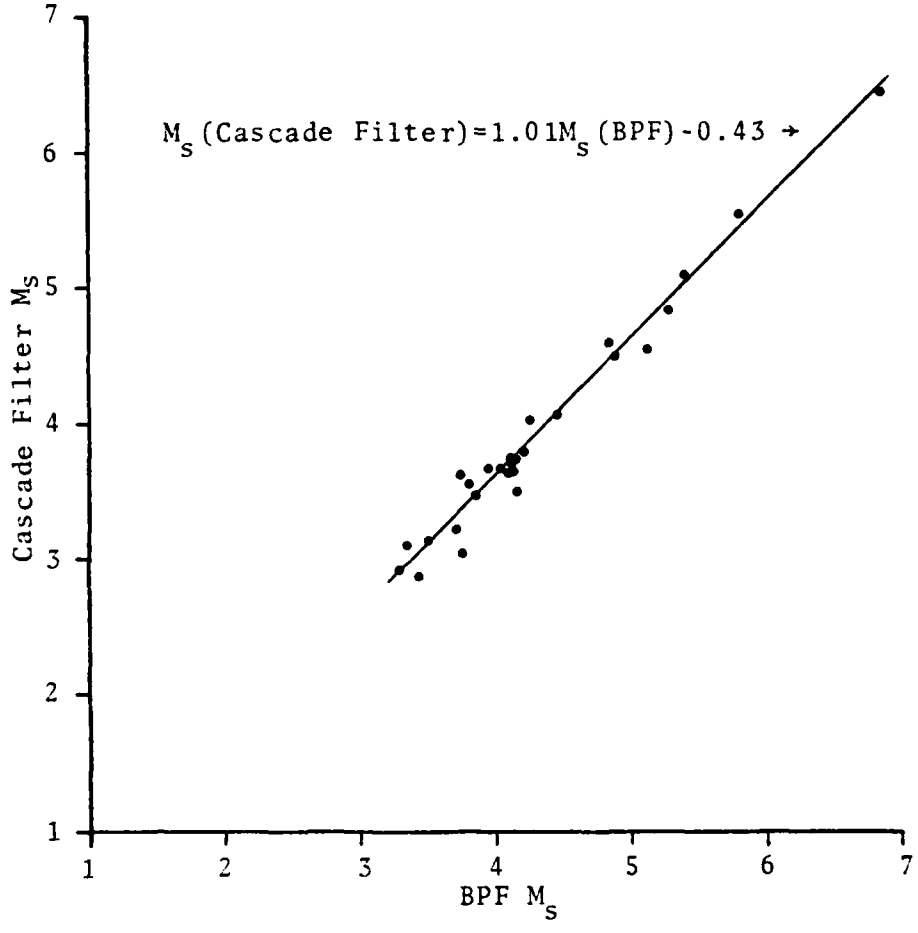

FIGURE V-3

COMPARISON OF M_s MEASURED ON BANDPASS FILTERED DATA TO M_s MEASURED ON CASCADED FILTERED DATA (NETWORK)

Figures V-1 through V-3 show that surface wave magnitudes measured after application of this cascaded filter sequence are comparable to the surface wave magnitudes measured after bandpass filtering. Since the least-mean-square-error fit to the data of these figures have slopes of approximately one and have intercepts of 0.4-0.5, one can see that the effect of cascade filtering on surface wave magnitudes is to lower the surface wave magnitudes by 0.4-0.5 units. Such effects would have to be taken into account in any application involving surface wave M_s values.

B. SINGLE STATION DISCRIMINATION TEST

To perform this test, surface wave magnitudes were measured for all ANTQ- and KONO-recorded events which were detected after bandpass filtering and for all events which were detected after cascaded filtering. (All magnitudes were measured on the vertical component Rayleigh wave.) In addition, nineteen presumed explosions (listed in Table V-1) were filtered, and surface wave magnitudes were measured for all detections. Inclusion of any given event in the presumed explosion list was based primarily on its epicenter location; i.e., any event with an epicenter at a known test site was included in the list.

The test consisted of plotting the M_s-m_b pairs, of computing a linear fit to the earthquake data points, and of computing the variance of the data points about this linear fit. The fit in each case was made using an algorithm which treats neither variable as dependent and which minimizes the distance between the points and the fitted line in a least-square sense.

TABLE V-1

PRESUMED EXPLOSIONS EXTRACTED FROM
NATIONAL EARTHQUAKE INFORMATION SERVICE

Event	Date	Origin Time	m_b	Latitude ^oN	Longitude ^oE
1	08/09/78	18.00.00	5.6	65.0	129.0
2	08/10/78	07.59.54	6.6	73.0	55.0
3	08/24/78	18.00.02	5.2	67.0	113.0
4	08/29/78	02.37.09	6.4	49.0	78.0
5	09/15/78	02.36.59	6.5	50.0	78.0
6	09/16/78	11.16.32	4.0	50.0	79.0
7	09/20/78	05.02.57	4.2	50.0	79.0
8	09/21/78	15.00.00	5.3	68.0	87.0
9	10/08/78	00.00.01	5.0	62.0	113.0
10	10/17/78	05.00.02	6.4	48.0	48.0
11	10/17/78	14.00.00	5.8	65.0	64.0
12	10/31/78	04.16.59	5.0	50.0	79.0
13	11/04/78	05.06.00	6.2	50.0	79.0
14	11/29/78	04.33.06	6.5	50.0	79.0
15	12/14/78	04.43.00	4.5	50.0	79.0
16	12/18/78	08.00.03	6.3	48.0	48.0
17	12/20/78	04.32.58	4.4	50.0	79.0
18	01/17/79	08.00.00	6.6	48.0	48.0
19	02/16/79	04.03.56	5.1	50.0	79.0

The dashed lines in each M_s-m_b plot in this section represent plus-or-minus two standard deviations about the fitted line. This measure will serve to classify the presumed explosions of Table V-1, since plus-or-minus two standard deviations about the mean of a normally-distributed population encloses 95 percent of the members of the population. Since explosions generate lower-magnitude surface waves than do earthquakes, the explosions should lie below the earthquake population. Therefore, this simple presentation scheme should mis-classify earthquakes as explosions in only 2.5 percent of the cases.

Figure V-4 presents the M_s-m_b plots determined from bandpass filtered data recorded at ANTO and KONO. The earthquake M_s-m_b data points are represented by solid circles (•) and the presumed explosion M_s-m_b points are represented by crosses (+). These figures show that only seven of the nineteen presumed explosions could be detected and classified based on the bandpass filtered data (all seven classify as explosions). One earthquake of the KONO data base also would be classified as an explosion based on this criterion. Note that only 15 percent of the ANTO earthquake data base and 21 percent of the KONO data base appear in these plots - all other earthquakes were not detected.

Figure V-5 presents the corresponding M_s-m_b plots determined from cascade filtered data recorded at ANTO and KONO. These plots show that fourteen of the presumed explosions as recorded at ANTO and eleven of the presumed explosions as recorded at KONO could be detected and classified. At both stations, however, two of these presumed explosions classify

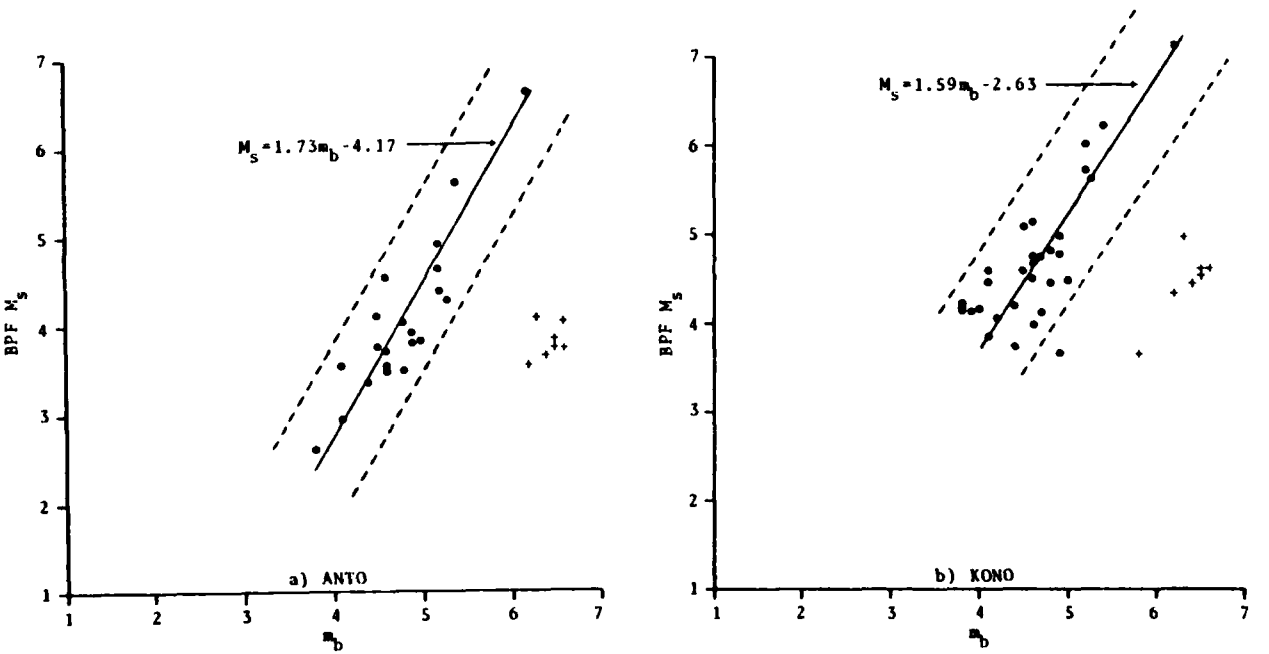

FIGURE V-4

M_s-m_b PLOTS FOR ANTO AND KONO; M_s MEASURED ON BANDPASS FILTERED DATA

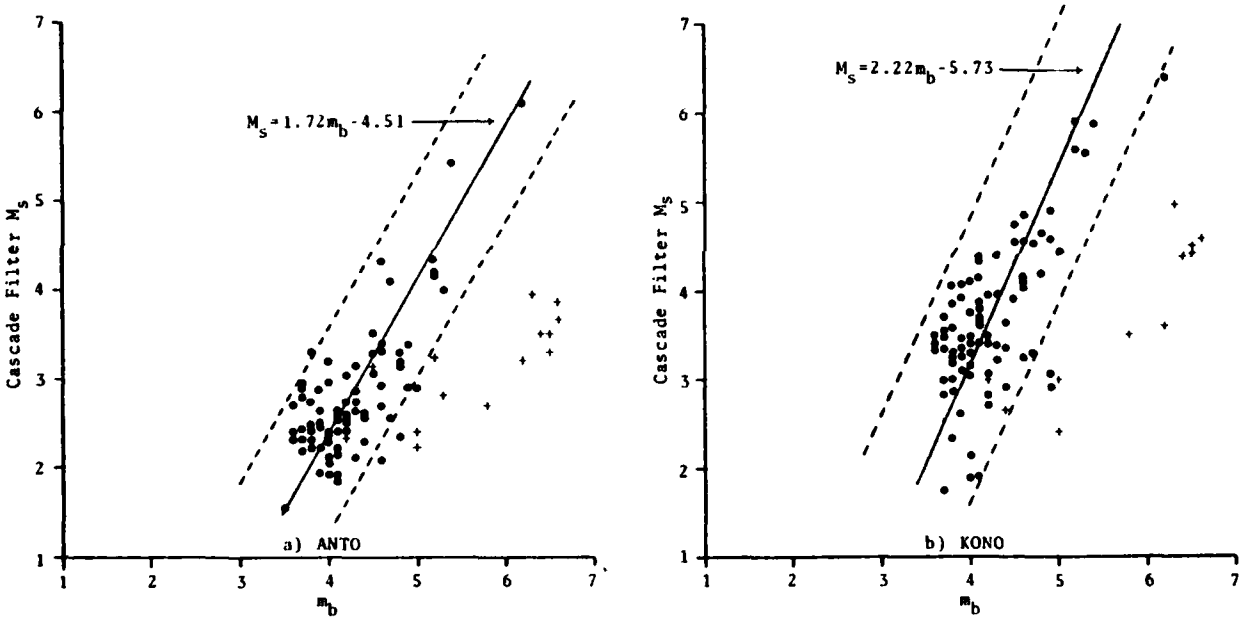

FIGURE V-5

M_s-m_b PLOTS FOR ANTO AND KONO; M_s MEASURED ON CASCADE FILTERED DATA

as earthquakes. Also, at both stations, three of the earthquakes would be classified as explosions. Note that the percentage of the ANTO data base appearing in the plot has increased to 52 percent while the percentage of the KONO data base appearing has increased to 60 percent.

Therefore, these M_s-m_b data show that signal extraction using a cascade filter sequence extends the utility of the M_s-m_b discriminant by increasing the number of events which are detected and may, as a consequence, be classified. Put another way, using the cascade filter sequence, a greater number of signals would be detected for discrimination analysis.

C. NETWORK DISCRIMINATION TEST

To perform this test, a subset of the original data base was first formed in order to reduce the processing time required. A total of 47 earthquakes were selected for inclusion in this subset together with the nineteen presumed explosions. Each signal as recorded at each station of the network was filtered by the bandpass filter/polarization filter/Gaussian narrowband filter cascade sequence and was examined for signal detections after application of the bandpass filter and after application of the cascade filter sequence. Surface wave magnitudes were then computed for each detected signal, and the individual station surface wave magnitudes were averaged to form the network magnitude. Finally, a restriction was placed on the data; for an event to be considered as detected, it must be detected on the data recorded by at least two stations. This restriction was imposed to minimize

the possibility of including 'surface wave magnitudes' which were actually measured on noise.

The results of this test are shown in Figure V-6. Figure V-6a shows the M_s-m_b data measured on the bandpass filtered data. Nineteen of the 47 earthquakes and ten of the nineteen presumed explosions had a sufficient number of detections after bandpass filtering to appear in this plot. Note that all ten of the presumed explosions classify as explosions.

Figure V-6b shows the M_s-m_b data measured on the cascade filtered data. In this case, 44 of the 47 earthquakes and all of the presumed explosions had sufficient detections to appear in the plot. Fifteen of the nineteen explosions classify as explosions while the remaining four events fall into the earthquake population. Note that one of the earthquakes classifies as an explosion.

Table V-2 summarizes the classification results for the nineteen events listed in Table V-1. This table shows that use of cascaded filters to extract signals greatly increases the number of events which can be detected, and, therefore, which are available for classification analysis.

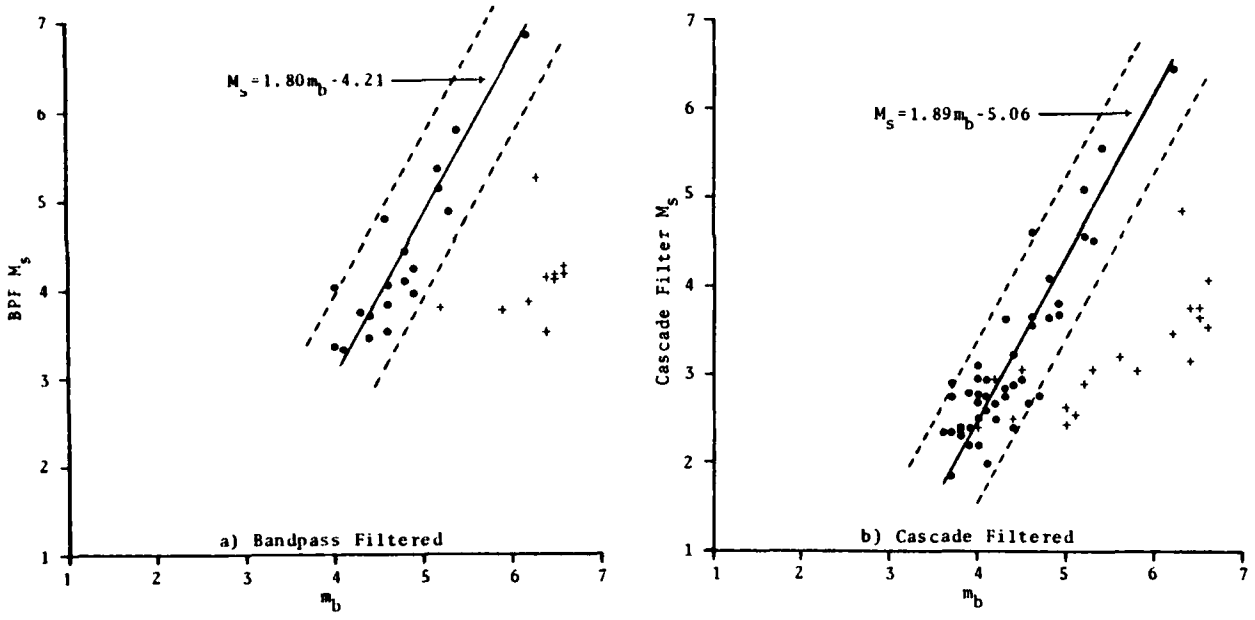

FIGURE V-6

NETWORK M_s-m_b PLOTS

TABLE V-2

SUMMARY OF DISCRIMINATION TEST

Event	ANTO		KONO		Network	
	Bandpass Filter	Cascaded Filters	Bandpass Filter	Cascaded Filters	Bandpass Filter	Cascaded Filters
1	-	-	-	-	-	X
2	X	X	-	-	X	X
3	-	X	-	-	X	X
4	-	-	-	-	X	X
5	X	X	X	X	X	X
6	-	-	-	-	-	E
7	-	E	-	E	-	E
8	-	X	-	-	-	X
9	-	X	-	X	-	X
10	X	X	X	X	X	X
11	-	X	X	X	X	X
12	-	X	-	X	-	X
13	X	X	X	X	X	X
14	X	X	X	X	X	X
15	-	E	-	-	-	E
16	X	X	X	X	X	X
17	-	-	-	E	-	E
18	X	X	X	X	X	X
19	-	-	-	-	-	X

- Event not detected; no classification possible

X Event classed as explosion

E Event classed as earthquake

SECTION VI
CONCLUSIONS

A. SUMMARY OF RESULTS

The follow conclusions are drawn from this study:

- An effective long-period signal extraction program has been created and tested on data recorded by Eurasian SRO stations. This program exists in both interactive and automatic mode versions.
- Both versions of the program are modularized for ease of insertion of additional signal extraction techniques.
- The polarization filter dominates the cascaded filter process. Cascaded filter sequences containing this filter yielded SNR gains of up to 14 to 15 dB.
- The bandpass filter/polarization filter/Gaussian narrowband filter cascade filter sequence produced an improvement in surface wave detection capability equivalent to approximately 0.6-0.8 m_b units.
- Cascade filtering enhanced the discrimination capability by increasing the number of detected signals for which reliable surface wave magnitudes can be estimated.

B. FEASIBILITY AND OPERABILITY OF APPLYING THE LONG-PERIOD SIGNAL EXTRACTION PROGRAM TO A LARGE WORLD-WIDE DATA BASE

Based on the results of this study, the most feasible approach to applying the long-period signal extraction program to a large world-wide data base would be to have both interactive mode and automatic mode versions resident on the same computer. This would permit one to process the majority of the data using the automatic mode, with the interactive mode reserved for parameter determination and the analysis of time segments of more than usual interest. (It is anticipated that attempts to use the interactive mode on all the data of a large data base would overwhelm the analyst. Automatic mode processing of the majority of the data should avoid this.)

Initially, it would be necessary to determine the signal suppression of each selected cascade filter sequence at each station providing data to the data base. This is necessary to permit computation of comparable surface wave magnitudes for events detected by different cascade filter sequences, since the degree of signal suppression varies with the choice of cascade filter sequence and the recording station (Table III-3).

C. SUGGESTED ADDITIONAL RESEARCH

Significant gains in detecting and measuring weak surface wave signals can be achieved by evaluating and optimizing

an alternate design for the cascade filter used in the signal editing process. The cascaded bandpass filter/polarization filter/Gaussian narrowband filter sequence (B_1, P, G; see Table III-1) evaluated in this study is considered the optimum choice of a processor which automatically edits and measures surface wave signals. It was designed for maximum-likelihood detection of at least 85% of the signals which are expected to be observed.

Another cascade configuration, the Wiener filter/polarization filter/chirp filter/Gaussian narrowband filter sequence (W, P, C, G), provides an enhanced capability for extracting weak, hard-to-detect signals which are missed by the B_1, P, G sequence. The capability of the W, P, C, G processor to detect weak signals at the 15% level of detection results from the higher variance associated with this processor. This is especially the case for the network-related performance of the W, P, C, G processor in that at least one additional detection out of the eight SRO stations used here is expected at the 15% level of detection.

For enhanced network performance, it is proposed that the W, P, C, G cascade filter sequence be operated in parallel with the B_1, P, G cascade filter sequence. Based on the statistics of Table III-1, it is expected that at least 0.17 units of improved magnitude detection capability can be achieved in this way for single-station detections. Considerably more gain is expected to be achieved when parallel processors are used with a network. This can be accomplished (with only a minor increase of computer time) by utilizing the W, P, C, G cascade filter sequence as a backup to the automated

B_1, P, G cascade filter sequence. In this dual mode of operation the W, P, C, G cascade filter sequence would be used only when signals are not detected after application of the B_1, P, G cascade filter sequence.

SECTION VII
REFERENCES

Flinn, E. A., and E. R. Engdahl, 1965; A Proposed Basis For Geographical and Seismic Regionalization; Reviews of Geophysics, Volume 3, Number 1, p. 123-149.

Harley, T. W., 1971; Long Period Array Processing Development Final Report; AFTAC Contract Number F33657-69-C-1063, Texas Instruments Incorporated, Dallas, TX.

Lane, S. S., 1976; Development of Three Signal Processing Techniques; Technical Report No. 6, Texas Instruments Report No. ALEX(01)-TR-76-06, AFTAC Contract Number F08606-76-C-0011, Texas Instruments Incorporated, Dallas, TX.

Lane, S. S., 1977; Extraction of Long-Period Surface Waves; Technical Report No. 8, Texas Instruments Report No. ALEX(01)-TR-77-08, AFTAC Contract Number F08606-77-C-0004, Texas Instruments Incorporated, Dallas, TX.

Ringdal, F., 1974; Estimation of Seismic Detection Thresholds; Technical Report No. 2, Texas Instruments Report No. ALEX(01)-TR-74-02, AFTAC Contract Number F08606-74-C-0033, Texas Instruments Incorporated, Dallas, TX.

Ringdal, F., J. S. Shaub, and D. G. Black, 1975; Documentation of the Interactive Seismic Processing System (ISPS); AFTAC Contract Number F08606-75-C-0029, Texas Instruments Incorporated, Dallas, TX.

Shaub, J. S., and D. G. Black, 1977; The Extended Interactive Seismic Processing System (ISPSE); Texas Instruments Report No. ALEX(01)-TR-77-09, AFTAC Contract Number F08606-77-C-0004, Texas Instruments Incorporated, Dallas, TX.

Snell, N. S., 1976; Network Capability Estimation; Technical Report No. 4, Texas Instruments Report No. ALEX(01)-TR-76-04, AFTAC Contract Number F08606-76-C-0011, Texas Instruments Incorporated, Dallas, TX.

Strauss, A. C., 1973; Final Evaluation of the Detection and Discrimination Capability of the Alaskan Long Period Array; Special Report No. 8, AFTAC Contract Number F33657-72-C-0725, Texas Instruments Incorporated, Dallas, TX.

Strauss, A. C., and A. I. Tolstoy, 1974; Evaluation of Matched Filters and the Three-Component Adaptive Processor for the VLPE Stations and the VLPE Network, Technical Report No. 5, Texas Instruments Report No. ALEX(01)-TR-74-05, AFTAC Contract Number F08606-74-C-0033, Texas Instruments Incorporated, Dallas, TX.

Strauss, A. C., 1976; Evaluation of the Improved Three-Component Adaptive Processor; Technical Report No. 7, Texas Instruments Report No. ALEX(01)-TR-76-07, AFTAC Contract Number F08606-77-C-0004, Texas Instruments Incorporated, Dallas, TX.

Strauss, A. C., and L. C. Weltman, 1977; Continuation of the Seismic Research Observatories Evaluation; Technical Report No. 2, Texas Instruments Report No. ALEX(01)-TR-77-02, AFTAC Contract Number F08606-77-C-0004, Texas Instruments Incorporated, Dallas, TX.

Strauss, A. C., 1978; Extraction of Seismic Waveforms; Technical Report No. 14, Texas Instruments Report No. ALEX(01)-TR-78-02, AFTAC Contract Number F08606-77-C-0004, Texas Instruments Incorporated, Dallas, TX.

Strauss, A. C., 1979; Application of the Phase-Difference Polarization Filter to Short-Period Regional Data; Technical Report No. 3, ENSCO Report No. SAR(01)-TR-79-03, AFTAC Contract Number F08606-79-C-0014, ENSCO Inc., Springfield, VA.

Weltman, L. C., H. Y. A. Hsiao, and R. R. Oliver, 1979; An Evaluation of the Seismic Research Observatories: Final Report; Technical Report No. 4, ENSCO Report No. SAR(01)-TR-79-04, AFTAC Contract Number F08606-79-C-0014, ENSCO Inc., Springfield, VA.